THE JOURNAL OF BIOLOGICAL CHEMISTRY
Vol. 279, No. 2, Issue of January 9, pp. 1491–1498, 2004
Printed in U.S.A.

Crystal Structure of Human Pirin

AN IRON-BINDING NUCLEAR PROTEIN AND TRANSCRIPTION COFACTOR*

Received for publication, September 9, 2003, and in revised form, October 13, 2003
Published, JBC Papers in Press, October 22, 2003, DOI 10.1074/jbc.M310022200

Hai Pang‡§, Mark Bartlam‡§, Qinghong Zeng‡§, Hideyuki Miyatake¶, Tamao Hisano¶, Kunio Miki¶, Luet-Lok Wong‖, George F. Gao‡, and Zihe Rao‡ ‡‡**

*From the ‡Laboratory of Structural Biology, Tsinghua University and National Laboratory of Biomacromolecules, Institute of Biophysics, Chinese Academy of Science, School of Life Sciences and Engineering, Beijing, Beijing 100084, China, the ¶Theoretical Structural Biology Laboratory, RIKEN Harima Institute, SPring-8, Hyogo 679-5148, Japan, the ‖Department of Chemistry, Inorganic Chemistry Laboratory, South Parks Road, Oxford OX1 3QR, United Kingdom, and the **Nuffield Department of Clinical Medicine, University of Oxford, John Radcliffe Hospital, Headington, Oxford OX3 9DU, United Kingdom*

Pirin is a newly identified nuclear protein that interacts with the oncoprotein B-cell lymphoma 3-encoded (Bcl-3) and nuclear factor I (NFI). The crystal structure of human Pirin at 2.1-Å resolution shows it to be a member of the functionally diverse cupin superfamily. The structure comprises two β-barrel domains, with an Fe(II) cofactor bound within the cavity of the N-terminal domain. These findings suggest an enzymatic role for Pirin, most likely in biological redox reactions involving oxygen, and provide compelling evidence that Pirin requires the participation of the metal ion for its interaction with Bcl-3 to co-regulate the NF-κB transcription pathway and the interaction with NFI in DNA replication. Substitution of iron by heavy metals thus provides a novel pathway for these metals to directly influence gene transcription. The structure suggests an interesting new role of iron in biology and that Pirin may be involved in novel mechanisms of gene regulation.

Pirin is a newly identified nuclear protein that is widely expressed in dot-like subnuclear structures in human tissues, in particular liver and heart (1). Pirins are highly conserved among mammals, plants, fungi, and even prokaryotic organisms and have been assigned as a sub-family of the cupin superfamily based on both structure and sequence homology (1, 2). The cupin superfamily is among the most functionally diverse of any protein family described to date, with both enzymatic and non-enzymatic members included (2). This cupin superfamily is grouped according to a conserved β-barrel fold and two characteristic sequence motifs. Study of Pirin reveals two cupin domains from its primary sequence that are consistent with other members of the superfamily.

The exact functions of Pirins are not yet known. No enzymatic activity has been described, but human Pirin has been found to bind to the nuclear factor I/CCAAT box transcription factor (NFI)[1] and to the oncoprotein B cell lymphoma 3-encoded (Bcl-3) *in vivo* (1, 3), suggesting that it is a transcription cofactor. NFI is known to stimulate DNA replication and RNA polymerase II-driven transcription (4). Bcl-3 is a distinctive member of the IκB family, which inhibits the transcription factor NF-κB by preventing NF-κB nuclear translocation and DNA binding. However, there is also evidence that Bcl-3 preferentially binds to NF-κB p50 or p52 homodimers to stimulate transcription (5). The functional nature of this difference between IκB (inhibiting) and Bcl-3 (enhancing) is not known, but it is clear that they bind to different protein partners. Pirin is one of four binding partners of Bcl-3, together with Bard1, Tip60, and Jab1, and can be sequestered into quaternary complexes with Bcl-3, p50, and DNA (3). These four Bcl-3-interacting protein partners, which do not share any sequence homology, might play some crucial role in regulating the function of Bcl-3 and IκB. Indeed, both Pirin and Bcl-3 are localized in the nucleus, and the potential roles of Pirin in NF-κB-dependent transcriptional regulation are implicated in a number of experiments (6–10).

Here we report the crystal structure of human Pirin to 2.1-Å resolution. Understanding of the Pirin structure is of critical importance in elucidating and understanding its function, in particular its interaction with the IκB family of proteins in its role as a transcription cofactor.

EXPERIMENTAL PROCEDURES

Cloning, Expression, Purification, and Crystallization—The complete gene fragment encoding human Pirin protein was subcloned into pET-28a expression vector from a human liver cDNA library, and the human Pirin was highly expressed as a soluble protein in *Escherichia coli* strain BL21(DE3) with a 6-residue His tag attached to its N terminus. Purification of the Pirin protein was carried out through an affinity chromatography Co-NTA His Bind column (Qiagen) followed by size-exclusion chromatography on a Superdex 75 column (Amersham Biosciences). Crystals of Pirin were grown using the hanging drop-vapor diffusion method from a solution containing 25 mg/ml Pirin in 14% polyethylene glycol 20000, 0.1 M MES, pH 6.5, at 16 °C. For phase determination, a selenomethionyl derivative was produced and crystallized under similar conditions. The Pirin crystals belong to the space group $P2_12_12_1$ with unit cell parameters a = 42.28, b = 67.12, c = 106.39 Å, $\alpha = \beta = \gamma = 90°$.

Structure Determination—Data sets were collected at three wavelengths from a single selenomethionine derivative crystal at 100 K on

* This work was supported by Grants G1999075600 (Project 973) and 2002BA711A12 (Ministry of Science and Technology, China) for the Human Structural Genomics Initiative. The costs of publication of this article were defrayed in part by the payment of page charges. This article must therefore be hereby marked "*advertisement*" in accordance with 18 U.S.C. Section 1734 solely to indicate this fact.

The atomic coordinates and structure factors (code 1J1L) have been deposited in the Protein Data Bank, Research Collaboratory for Structural Bioinformatics, Rutgers University, New Brunswick, NJ (http://www.rcsb.org/).

§ These authors contributed equally to this work.

‡‡ To whom correspondence should be addressed. Tel.: 86-010-6277-1493; Fax: 86-010-6277-3145; E-mail: raozh@xtal.tsinghua.edu.cn.

[1] The abbreviations used are: NFI, nuclear factor I; Bcl-3, B-cell lymphoma 3; MES, 4-morpholineethanesulfonic acid; AAS, atomic absorption spectrophotometry; r.m.s., root mean square; araC, 1-β-D-arabinofuranosylcytosine; Ni-ARD, nickel-binding dioxygenase, acireductone dioxygenase; 2-OG, 2-oxoglutarate.

TABLE I
Data collection and refinement statistics
The numbers in parentheses correspond to the highest resolution shell.

	MAD peak	MAD edge	MAD remote
Wavelength (Å)	0.9795	0.9799	0.9817
Resolution limit (Å)	50.0–2.1 (2.18–2.10)	50.0–2.1 (2.18–2.10)	50.0–2.1 (2.18–2.10)
Total reflections	95,485	95,271	94,836
Unique reflections	30,975	30,927	30,894
Completeness	90.5 (81.5)	90.4 (81.4)	89.9 (79.8)
R_{merge} [a]	5.0 (27.5)	5.0 (28.8)	5.0 (29.3)
I/σ (I)	7.3 (1.9)	7.0 (1.8)	6.8 (1.8)
Resolution range			50.0–2.1
R_{work} [b]			20.6
R_{free} [b]			24.9
Number of protein atoms			2,244
Number of water molecules			187
r.m.s. deviation			
Bonds (Å)			0.006
Angles (°)			1.35
Average *B* factor (Å^2)			
Protein			21.28
Water			29.35
Ramachandran plot			
Favored (%)			88.6
Allowed (%)			11.4

[a] $R_{merge} = \Sigma_h\Sigma_l|I_{ih} - \langle I_h\rangle|\Sigma_h\Sigma_I\langle I_h\rangle$, where $\langle I_h\rangle$ is the mean of the observations I_{ih} of reflection h.
[b] $R_{work} = \Sigma(||F_p(obs)| - |F_p(calc)||)/\Sigma|F_p(obs)|$; R_{free} = *R* factor for a selected subset (5%) of the reflections that was not included in prior refinement calculations.

beamline BL44B2 of SPring-8. Data were collected to 2.1-Å resolution using energies corresponding to the peak (λ_1 = 0.9795 Å) and edge (λ_2 = 0.9799 Å) of the experimentally determined selenium K-edge, and a low energy remote wavelength (λ_3 = 0.9817 Å). All processing, scaling, and merging of datasets were performed using the HKL2000 package (11). Initial phases were calculated to 2.5-Å resolution with SOLVE (12) from seven heavy atom sites, and RESOLVE (13) was used for density modification and phase extension to 2.1 Å. The Pirin model was built using ARP/wARP (14) and O (15) and was subsequently refined with CNS (16) using the low energy remote data. An initial round of simulated annealing was followed by alternate cycles of manual rebuilding and minimization. The final model contains 288 residues, 188 water molecules, and an Fe^{2+} ion. The position of the metal ion was evident as a peak greater than 16 σ in the $F_o - F_c$ map. The Fe^{2+} ion was refined at full occupancy with a temperature factor of 17.5 Å^2. The coordinating atoms His^{56} Nϵ2, His^{58} Nϵ2, His^{101} Nϵ2, and Glu^{103} Oϵ2 have temperature factors of 10.8, 18.1, 12.9, and 13.8 Å^2, respectively.

Identification of the Metal Ion—The metal ion bound in the N-terminal domain of Pirin was confirmed to be iron by atomic absorption spectrophotometry (AAS). The AAS experiments were performed in the Tsinghua Analysis Center using a Carl Zeiss Technology Analytic Jena AAS 6 Vario instrument. The presence of the metal ions Mg^{2+}, Ca^{2+}, Mn^{2+}, Fe^{2+}, Co^{2+}, Ni^{2+}, Cu^{2+}, and Zn^{2+} were analyzed. The results indicated that, after Co^{2+}-affinity chromatography, only Fe^{2+} remained in the protein solution after gel-filtration chromatography on a Superdex-75 column (Amersham Biosciences) and equilibration in 20 mM Tris-HCl (pH 8.0) and 150 mM NaCl.

RESULTS AND DISCUSSION

Structure Determination—The structure of human Pirin was determined using the multiple-wavelength anomalous dispersion method from a single selenomethionine derivative crystal. Details of the data collection and structure refinement are given in Table I. The asymmetric unit of the Pirin crystal contains one monomer. The electron density map is of high quality such that 288 out of 290 residues could be built. No density was observed for the two N-terminal residues, but the remainder of the Pirin molecule, including the C-terminal end of the polypeptide chain, is well defined (Fig. 1*a*). Two *cis*-proline residues could be identified in the structure (Pro^{31} and Pro^{50}). The final model of the structure contains 288 residues, 188 water molecules, and 1 Fe^{2+} ion. The presence of iron was established by atomic absorption spectrophotometry, and quantitative measurements showed that there is 1 mol of Fe^{2+} per mol of protein.

Structural Overview—Pirin is composed of two structurally similar domains arranged face to face (Fig. 1, *b* and *c*). The core of each domain comprises two antiparallel β-sheets, with eight strands forming a β-sandwich. The fold of each domain is very similar, and the two domains can be superimposed with an r.m.s. difference of 1.3 Å for 64 equivalent residues. The N-terminal domain (residues 3–134) additionally features four β-strands, and the C-terminal domain (residues 143–290) also includes four additional β-strands and a short α-helix. The two domains are cross-linked, with β1 forming part of one sheet of the C-terminal domain, and strands β25 and β26 forming an extension of one sheet of the N-terminal domain. The C-terminal α-helix packs against the outer surface of the N-terminal domain β-barrel. The two domains are joined by a short linker of 10 amino acids (residues 134–143) that contains a single turn of a 3_{10} helix. Four additional 3_{10} helices are located in the structure.

Similar cavities are found in each domain. In the N-terminal domain, the cavity contains a metal binding site with a single Fe^{2+} ion located at about 6 Å from the protein surface (Fig. 1*d*). The C-terminal domain cavity is more compact than the N-terminal domain and is closed by the β-strand formed by residues 6–12. The C-terminal domain does not contain any metal binding site.

Pirin Is a Member of the Cupin Superfamily—It has been predicted that Pirin belongs to the cupin superfamily on the basis of primary sequence (2). From a Dali (17) search for structural similarity, the Pirin structure was confirmed to closely resemble members of the cupin superfamily (Fig. 2, *a–f*), particularly the structures of quercetin 2,3-dioxygenase (18), glycinin g1 (19), and phosphomannose isomerase (20). As with Pirin, these three proteins are bicupins with two germin-like β-barrel domains. Pirin also contains the two characteristic sequences of the cupin superfamily, namely PG-$(X)_5$-H*X*H-$(X)_4$-E-$(X)_6$-G and G-$(X)_5$-P*X*G-$(X)_2$-H-$(X)_3$-N separated by a variable stretch of 15–50 amino acids (Fig. 2*g*). These motifs are best conserved in the N-terminal domain (residues 49–71 and residues 88–105) where the conserved histidine and glutamic acid residues correspond to the metal-coordinating residues. The C-terminal domain motifs (residues 178–199 and residues 216–230) lack the metal binding residues normally associated with the cupin fold.

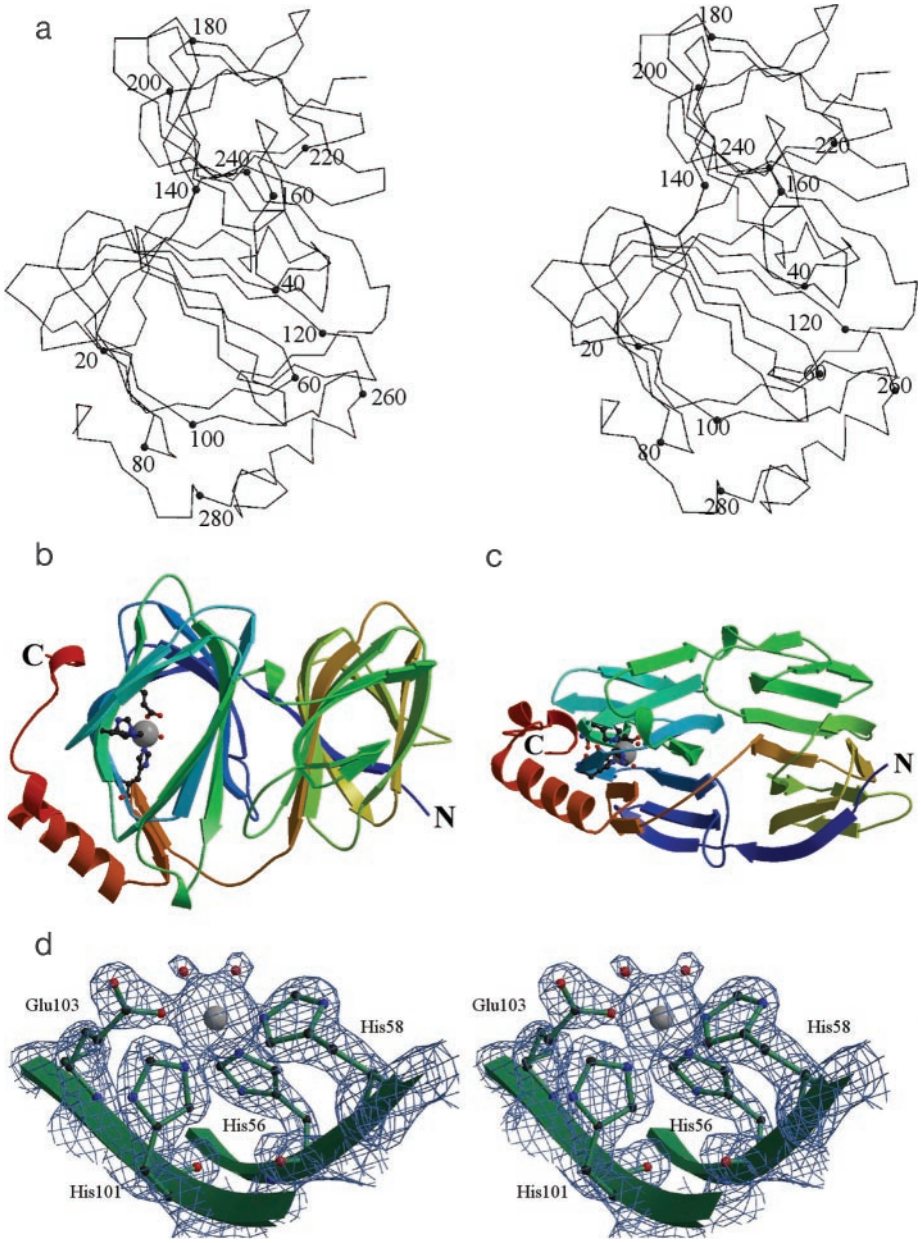

FIG. 1. **The Pirin structure.** *a*, a stereo diagram of the Pirin structure shown as a Cα trace. Every 20th residue is labeled. The *top view* (*b*) and *side view* (*c*) of the Pirin structure are shown. The structure is colored from N-terminal (*blue*) to C-terminal (*red*). The metal ion is shown as a *large gray sphere*, and the coordinating groups and water molecules are shown as *ball-and-stick models*. *d*, a stereo diagram showing the electron density map in the metal binding site. The metal ion is coordinated by three histidines, one glutamate, and two water molecules. The omit map is contoured at 1.8 σ.

The cupin superfamily has possibly the widest range of biochemical functions of any superfamily identified to date (2). It is comprised of both enzymatic and non-enzymatic members, which have either one or two cupin domains. The cupin fold comprises a motif of six to eight antiparallel β-strands located within a conserved β-barrel structure (2). The variety of biochemical functions is reflected by the low sequence homology shared among the cupin superfamily members (Fig. 2*g*). A BLAST search for proteins homologous to human Pirin revealed significant conservation between mammals, plants, and prokaryotes, particularly within the N-terminal domain (1). Interestingly, sequence alignment of human Pirin and related proteins reveals two clusters that are highly conserved throughout all aligned sequences. These sequence clusters, corresponding to residues 52–70 (cluster 1) and 88–106 (cluster 2), include the four metal coordinating residues of human Pirin, which are strictly conserved among all aligned sequences.

Pirin (Fig. 2*a*) and the bicupin metalloenzymes quercetin 2,3-dioxygenase (Fig. 2*b*) and phosphomannose isomerase (Fig. 2*d*) show similarities in the overall fold. Quercetin 2,3-dioxygenase is a copper-containing enzyme, and its N-terminal domain can be superimposed onto the N-terminal domain of Pirin with an r.m.s. difference of 1.5 Å for 84 equivalent residues. The Cu-binding site of quercetin 2,3-dioxygenase, formed by 3 histidines, a glutamic acid residue and a single water molecule, matches the metal site of Pirin. The three histidines of Pirin (His^{56}, His^{58}, and His^{101}) are structurally equivalent to those of quercetin 2,3-dioxygenase (His^{66}, His^{68}, and His^{112}). Similarly, the phosphomannose isomerase structure can be superimposed onto that of Pirin with an r.m.s. difference of 1.3 Å for 71 equivalent residues. Phosphomannose isomerase is a zinc-containing enzyme, and its metal binding site, comprising two histidines and two glutamic acid residues, also matches the metal site of Pirin.

Regardless of the overall structural similarity between its two domains, the C-terminal domain of Pirin shows interesting differences from the N-terminal domain. Notably, the C-terminal domain of Pirin does not contain a metal binding site and its sequence does not contain the conserved metal-coordinating residues. Several members of the cupin superfamily do not contain the metal-coordinating residues, including the transcription factor araC from *Escherichia coli* (21). araC is a single

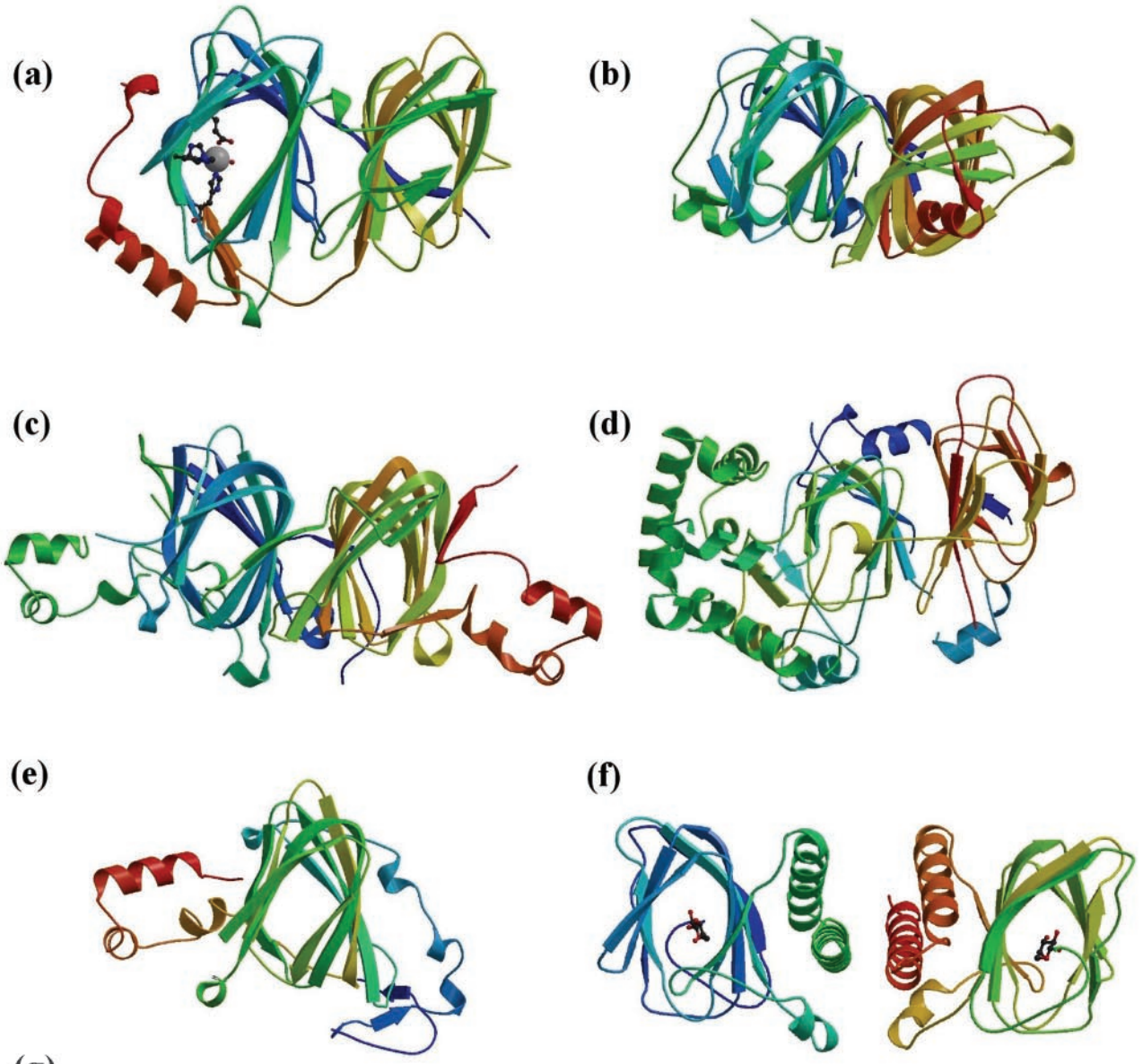

FIG. 2. **A comparison between Pirin and similar structures.** *a*, Pirin structure; *b*, quercetin 2,3-dioxygenase structure (PDB code: 1JUH); *c*, glycinin g1 structure (PDB code: 1FXZ); *d*, phosphomannose isomerase structure (PDB code: 1PMI); *e*, oxalate oxidase (germin) structure (PDB code: 1FI2); *f*, araC dimer structure (PDB code: 2ARC). *g*, structure-based sequence alignment of Pirin with related structures. *PIRIN-N*, N-terminal domain of Pirin; *PIRIN-C*, C-terminal domain of Pirin; *2,3QD-N*, N-terminal domain of quercetin 2,3-dioxygenase; *2,3QD-C*, C-terminal

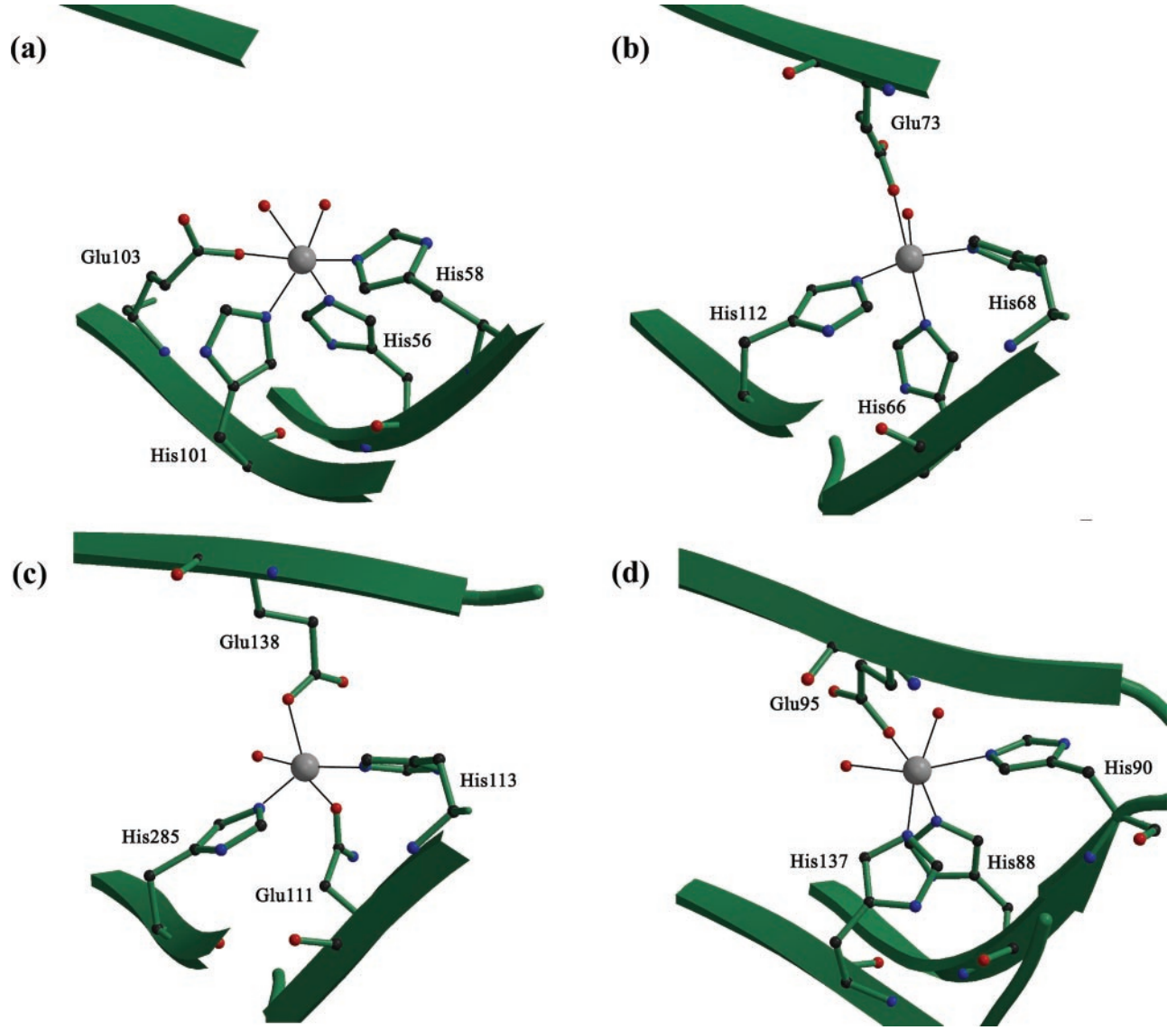

FIG. 3. **The metal binding site.** Metal binding sites of Pirin (*a*), quercetin 2,3-dioxygenase (PDB code: 1JUH, *b*), phosphomannose isomerase (PDB code: 1PMI, *c*), and oxalate oxidase (PDB code: 1FI2, *d*).

domain member of the cupin family and binds arabinose for activation of transcription. There are notable similarities between the C-terminal domain of Pirin and araC. In araC, the arabinose binding site is located within the β-barrel and is closed by an N-terminal domain arm. The β-barrel of the C-terminal domain of Pirin is also closed by the N-terminal β1 strand. However, in the absence of arabinose, the N-terminal arm of araC becomes disordered, suggesting that it is important for ligand stability. A detailed analysis of the arabinose binding residues in the araC structure shows that the C-terminal domain of Pirin is unlikely to bind arabinose.

The Metal Binding Site—Surprisingly, a single Fe^{2+} ion is located in the Pirin N-terminal domain where it is coordinated by 3 histidine residues (His^{56}, His^{58}, and His^{101}) through their Nϵ2 atoms, and one glutamic acid (Glu^{103}) through the Oϵ2 atom (Fig. 3*a*). The metal binding site is exposed to the solvent, and the octahedral coordination environment is completed by two water molecules, with metal-ligand distances of 2.24 and 2.15 Å (Table II). A structure-based sequence alignment shows that the metal binding motif is highly conserved within a number of other cupin superfamily members (Fig. 2*g*). The metal binding domain of Pirin is most structurally similar to that in germin, a Mn^{2+}-containing oxalate oxidase in which the metal is also octahedrally coordinated by three histidines, a glutamic acid and two water molecules (22). As with quercetin 2,3-dioxygenase, the three histidines in oxalate oxidase (His^{88}, His^{90}, and His^{137}) are structurally equivalent to those in Pirin (His^{56}, His^{58}, and His^{101}). One notable difference between Pirin and related metalloproteins of the cupin superfamily is the location of the coordinating Glu residue. Quercetin 2,3-dioxygenase (Fig. 3*b*), phosphomannose isomerase (Fig. 3*c*), and oxalate oxidase (Fig. 3*d*) all contain a conserved Glu residue in the equivalent structural position to residue 63 of Pirin. However, this residue is not conserved in Pirin and the coordinating Glu residue is instead located in position 103 on β-strand 10.

The structure of a nickel-binding dioxygenase, acireductone

domain of quercetin 2,3-dioxygenase; *PROGLYCININ*, glycinin g1; *PMI-N*, N-terminal domain of phosphomannose isomerase; *PMI-C*, C-terminal domain of phosphomannose isomerase; *OXALATE*, oxalate oxidase (germin); *ARAC*, araC. Only the regions adjacent to the two characteristic conserved cupin sequences are shown. The two conserved cupin sequence motifs are *shaded in gray*, and metal coordinating residues are shown in *green boxes*. The secondary structure elements relate to the Pirin N-terminal domain structure.

TABLE II
Metal-donor atom distances and temperature factors

	Distance to metal ion	Temperature factor
	Å	*Å²*
Fe^{2+}		17.5
His^{56} Nϵ2	2.07	10.8
His^{58} Nϵ2	2.12	18.1
His^{101} Nϵ2	2.32	12.9
Glu^{103} Oϵ2	2.28	13.8
Water 1	2.24	19.1
Water 2	2.15	22.4

dioxygenase (Ni-ARD) from *Klebsiella pneumoniae*, was recently determined by NMR and its active site modeled by comparative homology modeling (23). It was suggested that ARD might also be a member of the cupin superfamily. The Ni^{2+} ion in ARD was predicted to be coordinated by six ligands, namely three histidine residues, a glutamic acid, and two water molecules. The spatial arrangement of ligand groups in the Ni-ARD model is similar to that of Pirin and germin, with an average distance of 2.1 Å between the metal and donor atoms.

Potential Functions of Pirin—The bound metal ion may play an important role in Pirin function by stabilizing the N-terminal cupin domain structure and/or by imparting enzymatic activity to the protein. The iron found in the structure is the metal cofactor in numerous enzymes spanning a wide spectrum of activities.

Metal-dependent Transcriptional Regulation—Pirins are putative transcription cofactors. Heavy metals are known to play an important role in the transcriptional regulation of eukaryotic and prokaryotic genes (24–29). Pirin is newly identified in this study to be a metal-binding protein, and, interestingly, the metal-binding residues of Pirins are highly conserved across mammals, plants, fungi, and prokaryotic organisms. Pirin acts as a cofactor for the transcription factor NFI, the regulatory mechanism of which is generally believed to require the assistance of a metal ion (30). Our structural data support the hypothesis that the bound iron of Pirin may participate in this transcriptional regulation by enhancing and stabilizing the formation of the p50·Bcl-3·DNA complex. Metals have been implicated directly or indirectly in the NF-κB family of transcription factors that control expression of a number of early response genes associated with inflammatory responses, cell growth, cell cycle progression, and neoplastic transformation (30). However, most metal-dependent transcription factors are DNA-binding proteins that bind to specific sequences when the metal binds to the protein. Pirin, on the other hand, appears to function differently and bind to the transcription factor·DNA complex.

The His_3Glu ligand environment and octahedral geometry of the metal-binding site in Pirin are well suited for the binding of heavy metal ions. The Fe(II) cofactors in non-heme iron proteins such as Pirin are labile, and therefore substitution of iron in Pirin by other metal ions offers a novel mechanism by which heavy metals can directly interfere with gene transcription.

Potential Enzymatic Activity of Pirins—The Fe^{2+} binding site in Pirin closely resembles that found in germin, the archetypal cupin. Germin is a manganese-containing protein that has been shown to be an oxalate oxidase and superoxide dismutase (22, 31). We found that Pirin does not possess either superoxide dismutase or oxalate oxidase activity, but we cannot rule out oxidase activity with other substrates. Recently, a number of 2-oxoglutarate (2-OG)-dependent iron monooxygenases, including clavaminic acid synthase 1 (32), hypoxia-inducible factor (33, 34), and factor-inhibiting hypoxia-inducible factor, were suggested to be members of the cupin superfamily on the basis of sequence and structure homology (35). Pirin is structurally related to these enzymes, but 2-OG-dependent monooxygenases have a highly conserved H*X*(D/E) . . . H motif, with the two histidines and one aspartate or glutamate forming a facial triad, leaving three coordination sites on the octahedral Fe(II) center for the binding of 2-OG and oxygen. Because the metal binding site in Pirins has a highly conserved His_3Glu set of ligands, with only two potentially vacant coordination sites on the Fe(II), Pirins are unlikely to be 2-OG-dependent monooxygenases. The other members of the cupin superfamily thought to contain iron are dioxygenases, and a phylogenetic analysis of cupins placed Pirins in the same clade as cysteine dioxygenases (2). Dioxygenases require electron transfer cofactor proteins, and the genes encoding the various proteins of a dioxygenase system are generally grouped together into an operon. Although no open reading frames encoding such cofactor proteins have been found on either the 5′ or 3′ sides of the human Pirin gene (1), this aspect warrants further investigation.

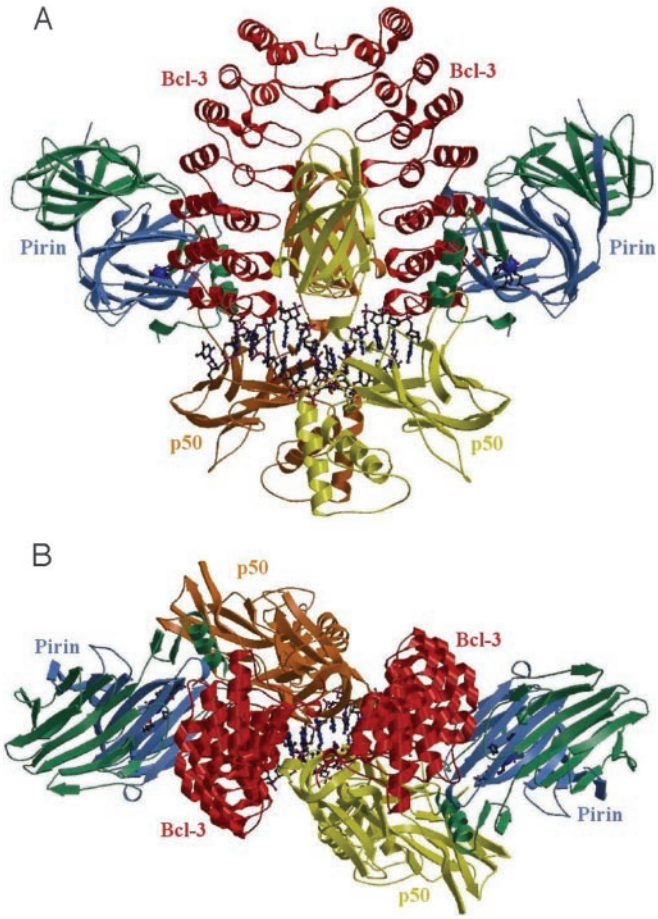

FIG. 4. **A model of the Pirin·Bcl-3·$(p50)_2$ complex (*A* and *B*).** The ankyrin repeat domain of Bcl-3 is shown as a *ribbon model colored red*. The Pirin structure is shown as a *ribbon model* with the N-terminal domain colored *blue* and the C-terminal domain colored *green*. The $(p50)_2$ homodimer is shown as a *ribbon model* with one p50 molecule colored *orange* and the other colored *yellow*.

Model of a Pirin·Bcl-3 Complex—The oncoprotein Bcl-3 is a distinctive member of the IκB family of NF-κB inhibitors and is located predominantly in the nucleus. It has the properties of a transcriptional co-activator and acts as a bridging factor between NF-κB/Rel and nuclear co-regulators. Pirin is known to be one of several binding partners that can associate with Bcl-3 (3) to form part of a larger quaternary complex on NF-κB DNA binding sites. Four binding partners of Bcl-3 have so far been identified, namely Pirin, Jab1, Bard1, and Tip60. There are no apparent shared sequence motifs in these four cofactors re-

quired for interaction with Bcl-3, and the only common properties between them is that they are nuclear proteins and associate with gene regulators.

The structure of the Bcl-3 ankyrin repeat domain (ARD) is elongated and is comprised of seven ankyrin (ANK) repeats (36). Its central ankyrin repeats are similar to those of IκBα, with the key difference that Bcl-3 has a seventh ankyrin repeat at the C terminus in place of the PEST region of IκBα. Mutagenesis studies of Bcl-3 indicated that all seven ankyrin repeats are required for binary interaction with Pirin, whereas interactions with Jab1 or Bard1 require only five repeats (3). Pirin and Bcl-3 can also be sequestered into quaternary complexes with p50 and DNA, and Pirin is known to increase the DNA binding by Bcl-3·p50. As with Pirin, all seven ankyrin repeats are required for the Bcl-3·p50 interaction (3). The stoichiometry of the complex is not known, but Bcl-3 is able to recognize at least two proteins simultaneously (3).

Because the structures of IκBα/NF-κB (p65/p50 heterodimer) (37, 38) complex and NF-κB p50 homodimer (39) are known, and to understand the interaction between Pirin, Bcl-3, and p50, we modeled the complex of these two proteins using protein-protein docking techniques (Fig. 4, *A* and *B*). A Bcl-3·$(p50)_2$ complex was constructed using the structures of the IκBα·NF-κB complex and the ankyrin repeat domain (ARD) of Bcl-3. The Bcl-3 ARD structure and the $(p50)_2$ homodimer were superimposed onto the IκBα·NF-κB complex. Pirin was then docked to the Bcl-3·$(p50)_2$ complex using the program FTDOCK (40). The surface of Pirin has a large acidic patch on the N-terminal domain surface formed by residues 77–82, 97–103, and 124–128. We suggest that this acidic patch could interact with the large basic patch on ankyrin repeats 6 and 7 of Bcl-3. Additional contacts to ankyrin repeat 5 of Bcl-3 could be formed by residues 160–166 of Pirin. Notably, the previous observation that Pirin binding to Bcl-3 requires all seven repeats of the ARD was based on C-terminal ARD deletion (ΔARD6–7 or ΔARD5–7) mutants, therefore, ARD4–7 of Bcl-3 might be the only domain interacting with Pirin (3), which is consistent with our model. Further analysis involving N-terminal ARD deletion mutants should provide further insight into the Pirin-Bcl-3 recognition interactions.

In our model of the complex, residues 265–284 of the C-terminal arm of Pirin could make contacts with one of the p50 molecules. One possibility is that Bcl-3 binding to the $(p50)_2$ homodimer could induce conformational changes that lead to Pirin binding to p50, although gel retardation experiments showed that there is no direct binding between Pirin and p50 (3). Although we emphasize that this model is only hypothetical, the extensive contacts formed by Pirin with Bcl-3 and p50 may explain why Pirin can act as a transcription cofactor and enhance the association of Bcl-3 with p50 homodimers.

Bcl-3 has a strong preference for p50 and p52 homodimers (3), and, under certain conditions, two molecules of Bcl-3 have been observed to bind to a single p50 or p52 homodimer (41). The addition of a second Bcl-3 molecule in our model, related to the first Bcl-3 molecule using the pseudodyad symmetry of the p50 homodimer, shows that the two Bcl-3 molecules have highly complementary hydrophobic contacts in the ankyrin repeats 1 and 2 (Fig. 4, *A* and *B*). IκBα, on the other hand, binds preferentially to p50-p65 heterodimers, and it is clear that the C-terminal of p65, containing the nuclear localization signal, would sterically hinder the binding of a second IκBα molecule. Our model gives some clues as to why Bcl-3 preferentially binds p50 or p52 homodimers and how p50 or p52 homodimers interact with Bcl-3.

Biological Implications—The structure of human Pirin represents the first crystal structure of the Pirin family and is an important step toward understanding the function of these proteins. Our work shows that human Pirin is a monomer with two cross-linked β-barrel domains. Pirin is confirmed to be a member of the cupin superfamily on the basis of primary sequence and structural similarity. The presence of a metal binding site in the N-terminal β-barrel of Pirin, which is highly conserved among Pirins, may be significant in its role in regulating NFI DNA replication and NF-κB transcription factor activity. Fe(II) was surprisingly found to be bound to Pirin and could impart enzymatic activity to the protein. Substitution of iron by other heavy metals also offers a direct mechanism for heavy metals to influence gene transcription. This novel pathway may be relevant in the toxicity and other effects of these metals. Finally, the structure of Pirin strongly suggests that a new role of iron in biology, namely regulating DNA replication and gene transcription at the level of the DNA complexes, should be added to the list of the many vital functions of this metal in living organisms.

Acknowledgments—We are grateful to Feng Gao, Fei Sun, and Zhiyong Lou from the Rao laboratory for assistance, and to Rongguang Zhang and Andrzej Joachimiak from the Advanced Photon Source (Argonne National Laboratory) for help with data collection. We thank Zhi Xing of the Tsinghua Analysis Center for help with atomic absorption spectrophotometry. Critical discussions with Neil Isaacs (Glasgow University, UK) and David Stuart (Oxford University, UK) are greatly appreciated.

REFERENCES

1. Wendler, W. M., Kremmer, E., Forster, R., and Winnacker, E. L. (1997) *J. Biol. Chem.* **272,** 8482–8489
2. Dunwell, J. M., Culham, A., Carter, C. E., Sosa-Aguirre, C. R., and Goodenough, P. W. (2001) *Trends Biochem. Science* **26,** 740–746
3. Dechend, R., Hirano, F., Lehmann, K., Heissmeyer, V., Ansieau, S., Wulczyn, F. G., Scheidereit, C., and Leutz, A. (1999) *Oncogene* **18,** 3316–3323
4. Santoro, C., Mermod, N., Andrews, P. C., and Tjian, R. (1998) *Nature* **334,** 218–224
5. Lenardo, M., and Siebenlist, U. (1994) *Immunol. Today* **15,** 145–147
6. Schwarz, E. M., Krimpenfort, P., Berns, A., and Verma, I. M. (1997) *Genes Dev.* **11,** 187–197
7. Richard, M., Louahed, J., Demoulin, J.-B., and Renauld, J. C. (1999) *Blood* **93,** 4318–4327
8. Bergman, A. C., Alaiya, A. A., Wendler, W., Binetruy, B., Shoshan, M., Sakaguchi, K., Bergman, T., Kronenwett, U., Auer, G., Appella, E., Jornvall, H., and Linder, S. (1999) *Cell Mol. Life Sci.* **55,** 467–471
9. Orzaez, D., de Jong, A. J., and Woltering, E. J. (2001) *Plant Mol. Biol.* **46,** 459–468
10. Mitchell, T. C., Hildeman, D., Kedl, R. M., Teague, T. K., Schaefer, B. C., White, J., Zhu, Y., Kappler, J., and Marrack, P. (2001) *Nat. Immunol.* **2,** 397–402
11. Otwinowski, Z., and Minor, W. (1997) *Methods Enzymol.* **276,** 307–326
12. Terwilliger, T. C., and Berendzen, J. (1999) *Acta Crystallogr. Sec. D* **55,** 849–861
13. Terwilliger, T. C. (2000) *Acta Crystallogr. Sec. D* **56,** 965–972
14. Perrakis, A., Morris, R., and Lamzin, V. S. (1999) *Nat. Struct. Biol.* **6,** 458–463
15. Jones, T. A., Zou, J. Y., Cowan, S. W., and Kjeldgaard, M. (1991) *Acta Crystallogr. Sect. A* **47,** 110–119
16. Brunger, A. T., Adams, P. D., Clore, G. M., DeLano, W. L., Gros, P., Grosse-Kunstleve, R. W., Jiang, J. S., Kuszewski, J., Nilges, M., Pannu, N. S., Read, R. J., Rice, L. M., Simonson, T., and Warren, G. L. (1998) *Acta Crystallogr. Sec. D* **54,** 905–921
17. Holm, L., and Sander, C. (1998) *Nucleic Acids Res.* **26,** 316–319
18. Fusetti, F., Schroeter, K. H., Steiner, R. A., Van Noort, P. I., Pijning, T., Rozeboom, H. J., Kalk, K. H., Egmond, M. R., and Dijkstra, B. W. (2002) *Structure* **10,** 259–268
19. Adachi, M., Takenaka, Y., Gidamis, A. B., Mikami, B., and Utsumi, S. (2000) *J. Mol. Biol.* **305,** 291–305
20. Cleasby, A., Wonacott, A., Skarzynski, T., Hubbard, R. E., Davies, G. J., Proudfoot, A. E., Bernard, A. R., Payton, M. A., and Wells, T. N. (1996) *Nat. Struct. Biol.* **3,** 470–479
21. Soisson, S. M., MacDougall-Shackleton, B., Schleif, R., and Wolberger, C. (1997) *Science* **276,** 421–425
22. Anand, R., Dorrestien, P. C., Kinsland, C., Begley, T. P., and Ealick, S. E. (2002) *Biochemistry* **41,** 7659–7669
23. Pochapsky, T. C., Pochapsky, S. S., Ju, T., Mo, H., Al-Mjeni, F., and Maroney, M. J. (2002) *Nat. Struct. Biol.* **9,** 966–972
24. DeMoor, J. M., and Koropatnick, D. J. (2000) *Cell Mol. Biol. (Noisy-le-grand)* **46,** 367–381
25. Makarova, K. S., Aravind, L., and Koonin, E. V. (2002) *Trends Biochem. Sci.* **27,** 384–386
26. Molkentin, J. D. (2000) *J. Biol. Chem.* **275,** 38949–38952
27. O'Halloran, T. V. (1993) *Science* **261,** 715–725
28. Fujita, M., Yamada, C., Goto, H., Yokoyama, N., Kuzushima, K., Inagaki, M., and Tsurumi, T. (1999) *J. Biol. Chem.* **274,** 25827–25832
29. Liang, R., Igarashi, H., Tsuzuki, T., Nakabeppu, Y., Sekiguchi, M., Kasprzak,

K. S., and Shiao, Y. H. (2001) *Ann. Clin. Lab. Sci.* **31,** 91–98
30. Chen, F., and Shi, X. (2002) *Environ. Health Perspect.* **110,** 807–811
31. Lane, B. G., Dunwell, J. M., Ray, J. A., Schmitt, M. R., and Cuming, A. C. (1993) *J. Biol. Chem.* **268,** 12239–12242
32. Zhang, Z., Ren, J., Stammers, D. K., Baldwin, J. E., Harlos, K., and Schofield, C. J. (2000) *Nat. Struct. Biol.* **7,** 127–133
33. Ivan, M., Kondo, K., Yang, H., Kim, W., Valiando, J., Ohh, M., Salic, A., Asara, J. M., Lane, W. S., and Kaelin, W. G., Jr. (2001) *Science* **292,** 464–468
34. Jaakkola, P., Mole, D. R., Tian, Y. M., Wilson, M. I., Gielbert, J., Gaskell, S. J., Kriegsheim, A., Hebestreit, H. F., Mukherji, M., Schofield, C. J., Maxwell, P. H., Pugh, C. W., and Ratcliffe, P. J. (2001) *Science* **292,** 468–472
35. Hewitson, K. S., McNeill, L. A., Riordan, M. V., Tian, Y. M., Bullock, A. N., Welford, R. W., Elkins, J. M., Oldham, N. J., Bhattacharya, S., Gleadle, J. M., Ratcliffe, P. J., Pugh, C. W., and Schofield, C. J. (2002) *J. Biol. Chem.* **277,** 26351–26355
36. Michel, F., Soler-Lopez, M., Petosa, C., Cramer, P., Siebenlist, U., and Muller, C. W. (2001) *EMBO J.* **20,** 6180–6190
37. Huxford, T., Huang, D. B., Malek, S., and Ghosh, G. (1998) *Cell* **95,** 759–770
38. Jacobs, M. D., and Harrison, S. C. (1998) *Cell* **95,** 749–758
39. Muller, C. W., Rey, F. A., Sodeoka, M., Verdine, G. L., and Harrison, S. C. (1995) *Nature* **373,** 311–317
40. Moont, G., Gabb, H. A., and Sternberg, M. J. E. (1999) *Proteins* **35,** 364–373
41. Bundy, D. L., and McKeithan, T. W. (1997) *J. Biol. Chem.* **272,** 33132–33139